Desalination and Water Treatment
www.deswater.com

doi: 10.1080/19443994.2014.941305

56 (2015) 1047–1055
October

Taylor & Francis
Taylor & Francis Group

Enhanced dyes removal properties of hollow SnO_2 Microspheres and SnO_2@C composites

Suzhen Ren*, Shaobo Ma, Ying Yang, Dongxu Tian, Hongmin Cai, Ce Hao

College of Chemistry, Dalian University of Technology, Dalian 116024, Liaoning, P.R. China, Tel. +86 411 84986074; emails: rensz@dlut.edu.cn (S. Ren), Mashb123@mail.dlut.edu.cn (S. Ma), Yangying632882@126.com (Y. Yang), tiandx@dlut.edu.cn (D. Tian), dreamflycai@163.com (H. Cai), Tel. +86 411 84986335; email: haoce@dlut.edu.cn (C. Hao)

Received 7 January 2014; Accepted 27 June 2014

ABSTRACT

SnO_2 hollow microspheres are controllably synthesized with the assistance of sulfonated polystyrene (sPS) colloidal spheres as hard templates. Via the interaction between ions of Sn^{2+} from the precursor $SnSO_4$ which are in ethanol–aqueous medium and -SO_3H ions on the template surface, sPS spheres-SnO_2 precursor (sPS@SnO_2) core–shell composite microspheres are prepared through a one-step hydrothermal method. The hollow SnO_2 microspheres can be obtained after removal of the sPS microspheres by calcination in air. Furthermore, SnO_2@C composite hollow spheres were fabricated with the further carbonization of the sPS@SnO_2@glucose composite microspheres. By scanning electron microscopy, transmission electron microscopy, and BET measurements; the morphology, specific surface area, and the core–shell structure were investigated. Application for hollow and composite spheres in sewage treatment of dye solution was evaluated. SnO_2 hollow spheres and SnO_2@C composite hollow spheres are adsorbent materials which can adsorb Congo red (CR), basic fuchsine, and methylene blue in solutions. SnO_2 hollow spheres can be simulated adsorption process of CR solution under acidic conditions. This process is regenerated and the regeneration performance is stable. The adsorption properties of SnO_2@C composite hollow spheres are improved than SnO_2 hollow spheres and they could be widely applied to sewage treatment.

Keywords: Template-assisted controllable synthesis; SnO_2 hollow sphere; Carbon-coated SnO_2 hollow sphere (SnO_2@C); Congo red; Dye removal; Wastewater treatment

1. Introduction

The development of an efficient, green, and low-cost method for removal of hazardous organic dye compounds is essential for the environmental protection. Various techniques for removing dyes from effluents have been developed, including electrochemical treatment, sonochemical treatment, photocatalytic oxidation and adsorption [1,2], etc. Among them, adsorption is a fast, inexpensive, and universal method for treatment of azo-containing effluents [1,2]. Consequently, many investigators have studied the feasibility of low-cost substances for adsorptive removal of various dyes, such as carbon material [3,4], and all kinds of metal oxides and hydroxides [2]. Although activated carbons have been most widely used for the adsorption of dyes, metal oxides, and

*Corresponding author.

hydroxides have been increasingly gaining attention because they are cheaper than activated carbons and they usually have chemical and mechanical stability, high surface area, and structural properties.

Currently, nanomaterials and nanotechnology have garnered worldwide attention for their application in environmental remediation and pollution control, because nanostructured surfaces offer large surface areas and rich valence states that provide enhanced affinity and adsorption capability toward pollutants [5–8]. For example, the development of various nanoscale tin oxides with uniform sizes for the removal of toxic heavy metal ions and organic pollutants from wastewater has accelerated recently, because of the low cost, abundant availability, and environmentally benign characteristics of these nanoscale materials [9–12]. Moreover, hollow nanostructures of spheres and multi-shell composite hollow spheres have demonstrated outstanding property of absorption of toxic heavy metal ions, compared with those of their bulk counterparts [12–16], and studies on the shape control synthesis of tin oxide nanostructures are actively being pursued [17–21].

Tin dioxide is the most thermodynamically stable phase of tin oxide. SnO_2 has been extensively used in catalysts, pigments, gas sensors, and energy storage [17–20,22,23]. We also have paid attention to synthesis of hollow SnO_2 microspheres with complex structures and large specific surface area. Recently, many studies of SnO_2 have been directed toward the fabrication of hollow SnO_2 spheres as promising adsorbents for water treatment [12]. These synthesis methods typically involve template-free routes, which result in hollow particles with a wide size distribution and nondefined shape. The common difficulties in template-based synthesis arise from creating uniform coatings of desired materials (or their precursors) on the surface of templates and maintaining their structural integrity after removal of templates. Moreover, controllable preparation of hollow particles with complex architectures, such as multi-shell structures, via a simple templating process still remains difficult. Therefore, it is highly desirable to be able to fabricate hollow SnO_2 in a simple, eco-friendly, and effective manner.

In this report, we describe a facile, green synthesis route for preparing hollow SnO_2 nanostructures via a template-assisted, hydrothermal method. This approach results in fine-controlled size and shape hollow products and is fast and energy efficient. A possible subsequent carbon coating process for the as-prepared hollow structures is conducted based on a glucose solution and heating treatment. With the hollow nanostructures and their wonderful intrinsic properties, the as-obtained hollow SnO_2 and SnO_2@C nanostructures exhibit excellent performance, with respect to the removal of Congo red (CR), basic fuchsine, and methylene blue from water.

2. Experimental section

2.1. Synthesis of hollow SnO_2 spheres and SnO_2@C composite

PS particles with different sizes were prepared by emulsion polymerization. Sulfonated polystyrene (sPS) was selected as template to coat SnO_2 shell. In typical route, 50 mg of prepared sPS spheres were dispersed in 10.0 mL of ethanol by ultrasonication firstly. Then, a small amount of polyvinylpyrrolidone (PVP) dissolved in water as surfactant was added to the sPS ethanol solution. Thirdly, freshly prepared 0.05 M $SnSO_4$ (10 mL) solution was added drop by drop and the solution was stirred for 8 h to form sPS@SnO_2 particles. Finally, these dried sPS@SnO_2 particles were transferred to furnace and calcinated (heating rate, 5 °C min^{-1}) at 550 °C under air for 2 h. Hollow SnO_2 particles were obtained.

SnO_2@C composites were fabricated as followed. 30 mg of sPS@SnO_2 spheres were dispersed in 4 mL of H_2O, 10 mL of ethanol, and 0.4 g of glucose. Then the mixture was transferred to the autoclave. The reaction temperature was 180 °C, and time was set to 15 h. After this reaction, sPS@SnO_2@C was obtained. In the next step, sPS@SnO_2@C was put into tube furnace and treated under N_2 for 4 h at 700 °C. The hollow SnO_2@C composite spheres were then obtained.

2.2. Characterization

Scanning electron microscopy (SEM) images was taken using a QUANTA 450 (FEI, America) apparatus. Transmission electron microscopy (TEM) was conducted together with energy dispersive X-ray spectrometer as its mode (Tecnai F30 with a field emission gun operating at 200 kV). X-ray diffraction (XRD) measurements of the as-prepared product were collected using a Bruker D8 Advance X-ray diffractometer with Cu Kα irradiation ($\lambda = 0.154$ nm) at room temperature. Nitrogen adsorption–desorption instrument (JW-BK112) was used to characterize the surface area and pore structure of the SnO_2 hollow spheres using N_2 sorption at 77 K. Surface area determination and pore analysis were performed using the BET method and the BJH method.

2.3. Adsorption behavior of CR

Congo red, which is an azo dye commonly used in the textile industry, was selected as a model organic

water pollutant. Various amounts of as-prepared hollow SnO_2 spheres were directly added to 50 mL of CR solution (0.10 g L^{-1}) under stirring. The hydrophilic membranes with the thickness of 0.45 μm were used for filtration and were prepared by complying with the following steps before each water treatment experiment: first, the filtration of 4 mL of a dye solution three times to make sure that the membranes could be saturated by the dye solution and then filtration by 4 mL of distilled water three times to eliminate the dye solution, and finally 4 mL of air several times until there is no residual distilled water. The CR solution was collected via 0.45 μm membranes at different time intervals. The concentration of CR in the solution was analyzed by UV–vis spectroscopy (Agilent Cary 5000, scan rate: 40 nm $min^{-1,}$ $\lambda max = 498$ nm).

3. Results and discussion

The observations of hollow spheres in SEM and TEM are summarized in Figs. 1 and 2. SEM images show that solid PS microspheres obtained by an emulsion polymerization process are monodispersive and the mean diameter is ca. 600 nm (Fig. 1(a)). The obtained PS spheres were treated by sulfonation using fume acid. The sulfonated polystyrene (sPS) was chosen as template microspheres for later coating reaction. The sPS@SnO_2 spheres from hydrothermal reactions are obtained by Sn^{2+} ions adsorbed on sPS surface react with H_2O molecules. The SnO_2 hollow spheres were prepared by removal of the sPS component as described previously [24,25]. The hollow SnO_2 nanoparticles have a mean diameter of about 550 nm. Some of the hollow spheres were deliberately broken to confirm that the spheres were hollow in Fig. 1(b). The microstructures of the SnO_2 spheres were further investigated by TEM. TEM images in Fig. 2 show the hollow and core shell structure of the SnO_2 spheres. Image in Fig. 2(a) indicates that the sPS@SnO_2 sample is mainly composed of bright core and dark coarse shell with thickness of 20–50 nm. After coating on these sPS@SnO_2 spheres surface with carbon (in Fig. 2(b)), these particles turn very slightly bigger than before coating and change into pale in the presence of a layer of carbon. Image in Fig. 2(c) is the hollow SnO_2@C composite particles from the removal of sPS in Fig. 2(b) by calcination treatment. The detailed observations shown in Fig. 2(d) and (e) reveal that there is a carbon layer with a thickness of 20 nm at the edge of SnO_2 architecture, which is pale white and transparent. Interesting comparison with high-magnification image in Fig. 2(f) without carbon coating, images in Fig. 2(d) and (e) show clearly that hollow SnO_2@C composite particles are formed. The effect of carbon layer on adsorbent behavior will be discussed below.

Fig. 3 presents an XRD pattern of a product. Except that sPS@SnO_2 microspheres before calcination (curve a in Fig. 3), all diffraction peaks can be attributed to the rutile-type tetragonal phase of SnO_2, in accordance with the standard JCPDS card (No. 41-1445). No other peaks resulting from reactants or intermediate phases were observed, indicating that hollow SnO_2 spheres were formed with high crystallinity and purity. The XRD pattern of the final SnO_2 hollow microspheres means that the calcination and removal of the sacrificial sPS template essentially leave the crystallinity unaffected. Based on the Scherrer

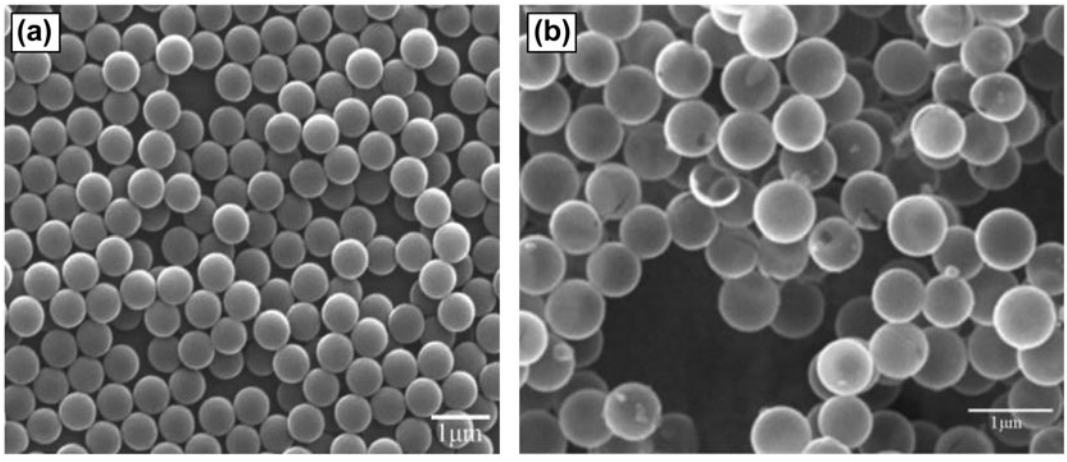

Fig. 1. SEM images of PS (a) and SnO_2 hollow spheres (b) (sPS@SnO_2 core shell particles heat treated 550°C under air for 8 h).

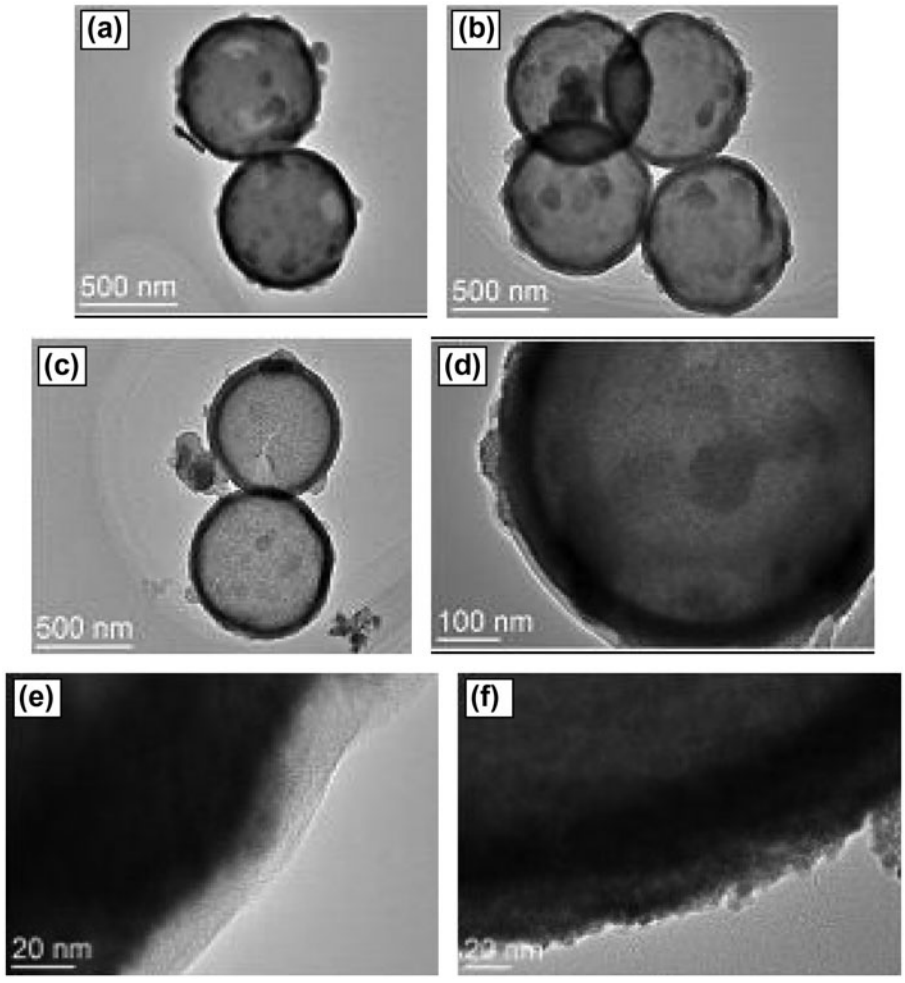

Fig. 2. TEM images of sPS@SnO_2 (a, f), sPS@SnO_2@C (b), and SnO_2@C (c, d, e).

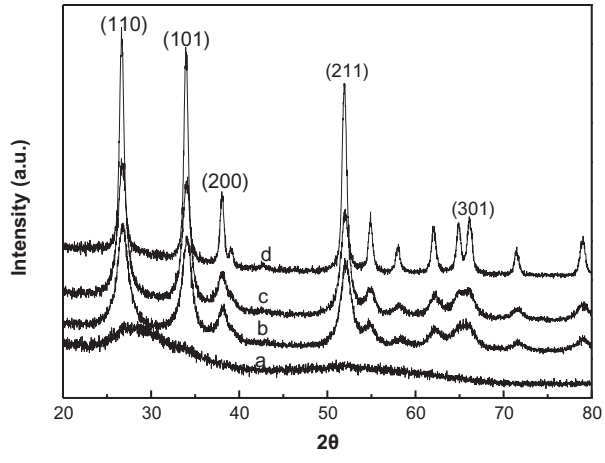

Fig. 3. XRD patterns of sPS@SnO_2 core–shell microspheres before calcination (a) and hollow SnO_2 spheres after calcination at different temperature: 550℃ (b), 650℃ (c), and 750℃ (d).

equation, $D = (0.89\lambda)/\beta(\cos\theta)$, where λ is the wavelength for the Kα(0.154 nm), β is the peak width at half-maximum in radians, and θ is the Bragg angle, the average particle size of the product treated at 550℃ (curve a) was calculated to be 7.3 nm. The particle size result is consistent with further high surface areas for adsorption of dyes.

The surface area and pore size distribution of the hollow SnO_2 and SnO_2@C composite nanostructures were further determined by nitrogen adsorption–desorption measurements. Fig. 4 shows N_2 adsorption–desorption isotherm of SnO_2 hollow spheres (Fig. 4(a)) and SnO_2@C composite hollow spheres (Fig. 4(b)). It shows a typical type IV isotherm with a hysteresis loop in the relative pressure range of 0.3–0.95, which suggests that the as-obtained spheres are mesoporous materials. The specific surface area of SnO_2 hollow nanoparticles, obtained by BET analysis, was 34.85 $m^2 g^{-1}$, and the mean pore diameter was

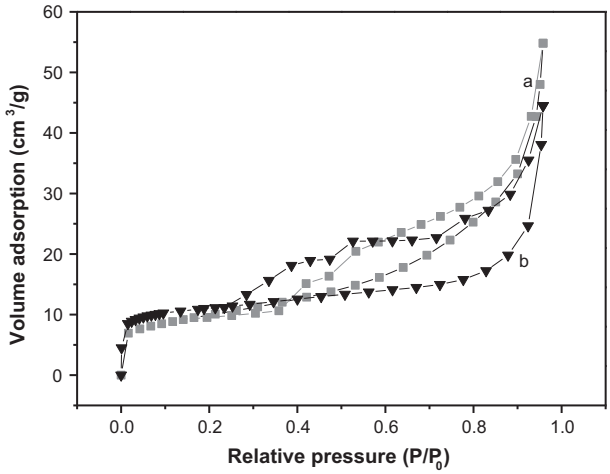

Fig. 4. Nitrogen adsorption–desorption isotherm of SnO_2 hollow spheres (a) and SnO_2@C composite hollow spheres (b).

9.39 nm and the specific surface area of SnO_2@C composite hollow particles was 44.92 $m^2 g^{-1}$, and the mean pore diameter was 12.99 nm, respectively, which are notably high values for tin oxide hollow nanostructures. These pores likely resulted from the void space between the interconnected nanospheres and in internal hollow spheres. This high surface area would be very beneficial for adsorbing and removing organic contaminant.

Inspired by their high BET surface areas originated from hollow and porous nanostructure, we expect that excellent absorbents for water treatment can be obtained. Furthermore, hollow SnO_2 and SnO_2@C building units bear a robust mechanical strength, and SnO_2 assemblies are environmentally friendly and can be recovered efficiently through a calcination process. These merits are very important for practical application in water treatment from an economic perspective.

Here, we investigated the potential application of the as-prepared hollow spheres to be used as an adsorbent in wastewater treatment. CR was chosen as a typical organic contaminant in the wastewater because it is often used as a dye in the textile industry. CR is typically absorbed onto the surface of metal oxides by coordination effect between metal ions and the amine groups at the ends of CR molecules. Fig. 5 shows the adsorption spectra of CR aqueous (with an initial concentration of 0.10 g L^{-1}) in the presence of SnO_2 hollow spheres at different dosage after treatment for 24 h. The absorption of CR at approximately 498 and 665 nm was used to monitor the process of adsorption. We can see that the intensity of the 498 nm peak decreased once the amount of SnO_2 hollow spheres was increased in Fig. 5(a) and (b) and surprisingly, after only 0.25 g

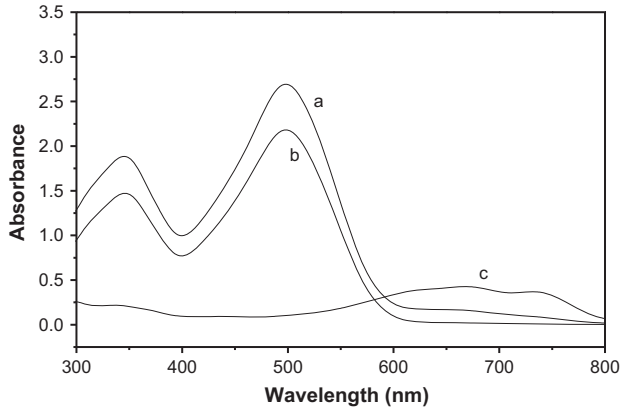

Fig. 5. UV–vis spectra of CR aqueous in the presence of SnO_2 hollow spheres at different dosage. (a) 0 g, (b) 0.05 g, (c) 0.25 g after adsorbation of 24 h. Volume of CR aqueous: 50 mL; initial concentration: 0.1 g L^{-1}.

SnO_2 in 50 mL CR, this peak completely vanished in 498 nm and shifted to mainly 665 nm and became weaker in observation (in Fig. 5(c)), suggesting the high efficiency for removing CR molecules. Further absorbent performance is marked in peak of 665 nm and this blue shift from 498 nm is discussed below.

The detailed measurement of absorption efficiency with different absorption time is show in Figs. 6–8. Fig. 6 is derived from Figs. 7 and 8. UV–vis spectra of CR aqueous (with an initial concentration of 0.10 g L^{-1}) in the presence of 0.5 g (Fig. 7) and 1 g (Fig. 8) SnO_2 hollow spheres at different intervals are clearly recorded. The effect of contact time on the adsorption

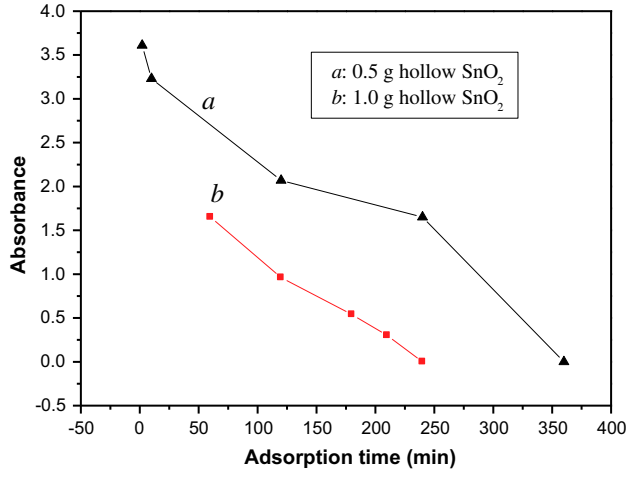

Fig. 6. Adsorption behavior of hollow SnO_2 spheres 0.5 g (curve a) and 1.0 g (curve b) in 50 mL 0.10 g L^{-1} CR solutions.

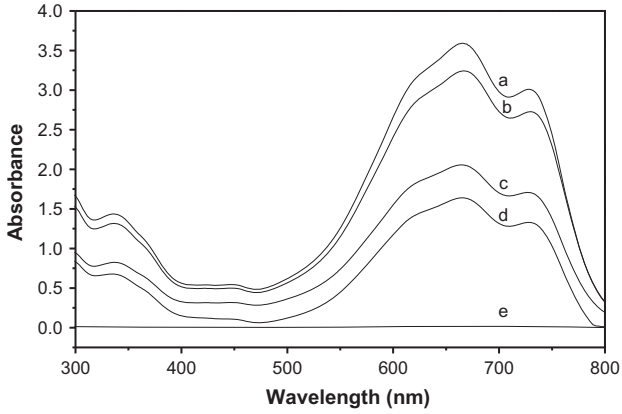

Fig. 7. UV–vis spectra of CR aqueous in the presence of 0.5 g SnO_2 hollow spheres at different intervals. (a) 2 min, (b) 10 min, (c) 2 h, (d) 4 h, (e) 6 h.

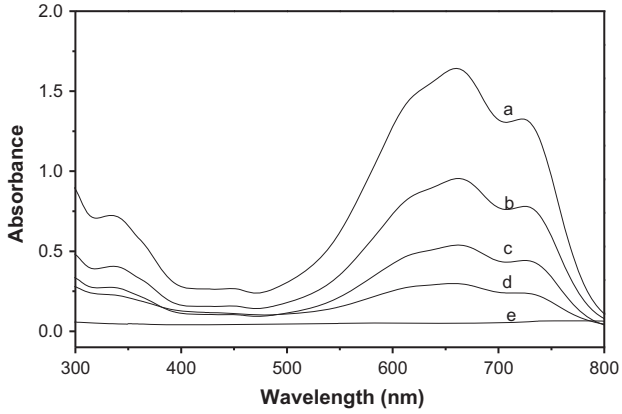

Fig. 8. UV–vis spectra of CR aqueous in the presence of 1 g SnO_2 hollow spheres at different intervals. (a) 1 h, (b) 2 h, (c) 3 h, (d) 3.5 h, (e) 4 h.

of CR was investigated to follow the adsorption process. When a 0.5 g of SnO_2 hollow nanoparticles was added into a 50 mL of CR solution (curve *a* in Figs. 6 and 7), absorbance of the solution at 665 nm decreased with the adsorption time increased. It can be seen that in about 4 h, it became about 50% adsorption. Almost for 6 h, there is no appearance of adsorbance shown, implying that adsorbents are valid for 6 h. When a 1.0 g of SnO_2 hollow nanoparticles was added into a 50 mL of CR solution (curve *b* in Figs. 6 and 8), it can be seen that for about 4 h, non-adsorbing tracer was tested implying that adsorbents were valid for 4 h.

Further experiments were carried out to compare the adsorption activity of the as-prepared SnO_2 hollow spheres with solid SnO_2 particles. Fig. 9 shows the adsorption efficiency of CR verse reaction time for

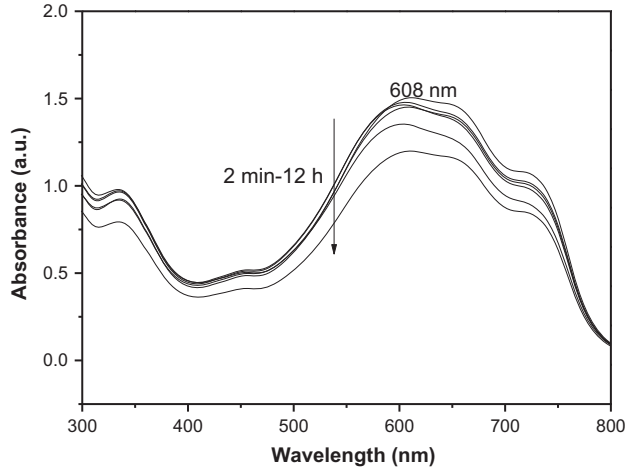

Fig. 9. UV–vis spectra of CR aqueous in the presence of 1 g SnO_2 solid particles from 2 min to 12 h.

solid SnO_2 particles. Here, the intensity of adsorption peak in 665 nm was similar as the time interval longer and changed very slightly, even after 12 h, indicting clearly that the solid SnO_2 spheres show lower adsorption efficiency than that of hollow materials. This should be induced by the much smaller surface area resulted from the solid spheres structure.

It is well known that the surface area and surface functional groups are two key factors in the adsorption capability of nanomaterials [26–30]. A large surface area can provide more active sites on which to absorb dye molecules, and the surface functional groups may interact with dye molecules by hydrogen bonds and/or electrostatic forces. CR is one acid dye with NH_2 groups. SnO_2 has a large number of SO_4^{2-} groups and basic sites on its surface. In this regard, SnO_2 may interact with the NH_2 of dye molecule via S–O···H–N and S–O–H···N hydrogen bonds and/or basic sites via electrostatic forces with an amino cation (NH_3^+). From the result in Fig. 4, our SnO_2 nanostructures have a relatively larger surface area of 12.99–45 $m^2 g^{-1}$. Therefore, their prominent adsorption capability may be largely ascribed to specific surface area. The hollow or broken hollow architectures cannot only provide more sites on which to absorb CR molecules but also facilitate the diffusion of CR molecules to the inside of SnO_2 nanostructures and thus enhance the absorption performance. There are abundant SO_4^{2-} groups on the surface of SnO_2 nanostructures. They will absorb CR molecules via a hydrogen bond, which arises from the interaction between SO_4^{2-} on the SnO_2 surface and NH_2 on the CR molecule surface. However, mainly due to the interaction between SO_4^{2-} on the SnO_2 surface and NH_2 on the CR molecule surface, there exists blue shift of the absorption wavelength.

There is another explanation for the blue shift of the 498 nm peak to 665 nm. Li et al. [31] and our lab [23] reported that there were oxygen vacancies on the surface on SnO_2 particles. Oxygen vacancies in the SnO_2 nanocrystals had effects on the electrochemical-improved performance when SnO_2 used as an anode material for lithium ion batteries [31]. We reported that oxygen vacancies in SnO_2 hollow shells had different redox performance from solid particles using H_2 TPR method [23]. However, mainly due to the interaction between oxygen vacancies on the SnO_2 surface and functional groups on the CR molecule surface, there exists blue shift of the absorption wavelength.

Therefore, the specific surface area of hollow structure, the electrostatic attraction between the SnO_2 surface and the CR species, and oxygen vacancies on surface could be responsible for such efficient removal of dye molecules. The high adaptability for hollow SnO_2 nanostructures in removing CR is attributed to their large surface area, surface SO_4^{2-} groups. Besides, it could be extended to other dyes with NH_2 groups in wastewater treatment. Figs. 10 and 11 show UV–vis spectra of basic fuchsine and methylene blue trihydrate aqueous in the presence of 1 g SnO_2 hollow spheres at different intervals, respectively. On the basis of the results, the SnO_2 has excellent absorption behavior on other dyes due to the specific structure of hollow SnO_2.

Fig. 12 UV–vis spectra of CR aqueous in the presence of 1 g SnO_2@C composite hollow spheres at different intervals from 10 min to 3 h. There is no blue shift of the maxima peak in 498 nm due to a thick layer of carbon, decrease of the concentration of SO_4^{2-} on the surface and oxygen vacancies. The absorb intensity deceases slowly with the adsorb time interval increases. It can be seen that it all desorbed after 3 h, implying that higher adsorbance efficiency due to higher specific surface area and surface functional groups.

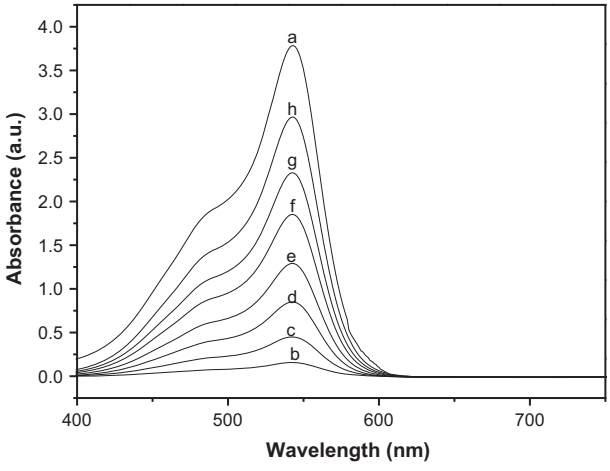

Fig. 10. UV–vis spectra of basic fuchsine aqueous in the presence of 1 g SnO2 hollow spheres at different intervals. (a) 0 min, (b) 10 min, (c) 20 min, (d) 30 min, (e) 1 h, (f) 2 h, (g) 3 h, (h) 4 h.

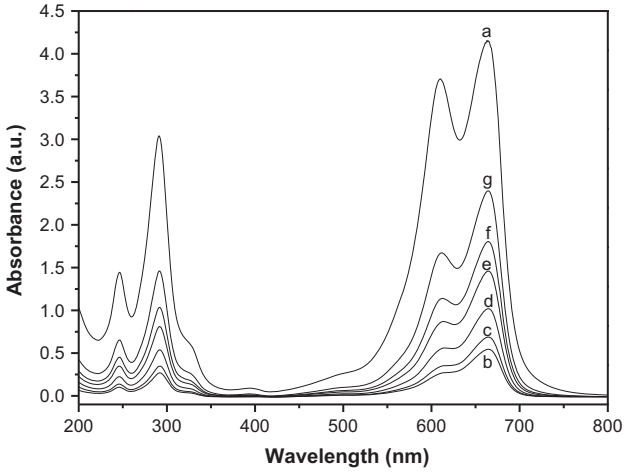

Fig. 11. UV–vis spectra of methylene blue trihydrate aqueous solution in the presence of 1 g SnO_2 hollow spheres at different intervals. (a) 0 min, (b) 10 min, (c) 20 min, (d) 30 min, (e) 1 h, (f) 2 h, (g) 4 h.

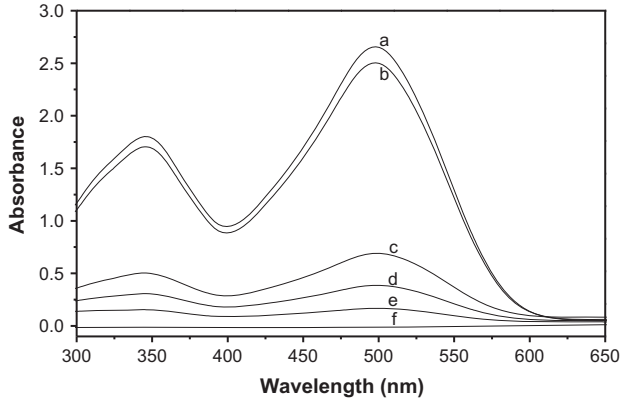

Fig. 12. UV–vis spectra of CR aqueous in the presence of 1 g SnO_2@C composite hollow spheres at different intervals. (a) 0 min, (b) 10 min, (c) 1 h, (d) 2 h, (e) 2.5 h, (f) 3 h.

Different SnO_2 adsorbents with various morphology need a comparison of absorption time for gauging our samples. Table 1 provides the absorption efficiency of different SnO_2-based absorbents on their absorption time when the absorption UV–vis spectra are non-detectable. From Table 1, it can be seen that hollow SnO_2 has an interval of 6 h in 1.0 g dosage

Table 1
Comparison of adsorption intervals for the adsorption of CR aqueous in the presence of adsorbents

	Hollow SnO_2 (g)					SnO_2 particles (g)	SnO_2@C (g)
Adsorbents	0.05	0.25	0.5	1.0	2.0	1.0	1.0
Adsorption interval (h)	24	24	6	4	2.5	12	3

while solid particles have 12 h. In addition, SnO_2@C has 3 h interval. Based on the Table 1, both the hollow SnO_2 and SnO_2@C have excellent absorption behavior on CR dye.

Regeneration of adsorbents in water treatment is one of the crucial aspects as it controls the economy of water treatment technology [2]. Regeneration of hollow SnO_2 spheres after adsorption of CR dye was investigated by centrifugation and separation followed by calcination in air for 4 h at 280˚C. The regenerated adsorbents reused for further adsorption CR successfully. Fig. 13 shows the good efficiency of this adsorbent after three cycles of adsorption/desorption processes. The adsorption time can be 5, 5.5, and 3 h (mainly in 498 nm) in first, second, and third cycle, respectively. These results indicated that nanoparticles could be regenerated and used for water treatment, which made these particles as economic tools. This property of nanoparticles may be considered as an extra advantage for their popularity in wastewater treatment.

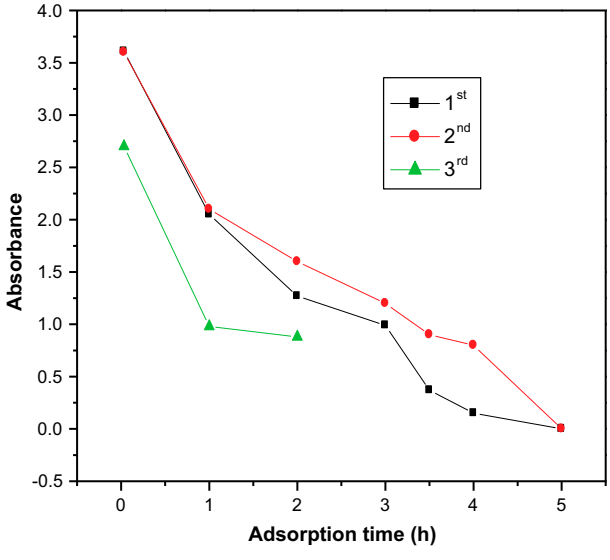

Fig. 13. Comparison of absorbance of CR aqueous in the presence of the first (a), second (b), and third (c) regenerated SnO_2 hollow spheres at different intervals.

4. Conclusions

Direct fabrication of hollow SnO_2 spheres has been carried out via template-assisted synthesis with a solution-phase route. The morphology, structure, and composition were systematically characterized by SEM, XRD, TEM, and CR absorption. The size of these hollow smooth spheres is in a range of 500–600 nm. Surfaces coating of carbon is found to be covered, which is believed to decrease the SO_4^{2-} groups on SnO_2 surface. The hollow SnO_2 spheres and SnO_2@C composites were used as adsorbent for the removal of typical azo dye (congo red, basic fuchsine, and methylene blue) from aqueous solution. The adsorbent dosage, contact time, and morphology on the adsorption played a significant role in the dye adsorption capacity of hollow SnO_2 spheres. The as-prepared SnO_2 hollow spheres were found to exhibit excellent adsorption performance of CR in aqueous solution, and they are expected to be employed in wastewater treatment for environmental cleaning.

Acknowledgments

This work was supported by the National Natural Science Foundation of China [grant number 21036006, 21137001].

References

[1] I. Ali, V.K. Gupta, Advances in water treatment by adsorption technology, Nat. Protoc. 1 (2006) 2661–2667.
[2] I. Ali, New generation adsorbents for water treatment, Chem. Rev. 112 (2012) 5073–5091.
[3] I. Ali, The quest for active carbon adsorbent substitutes: Inexpensive adsorbents for toxic metal ions removal from wastewater, Sep. Purif. Rev. 39 (2010) 95–171.
[4] I. Ali, M. Asim, T.A. Khan, Low cost adsorbents for the removal of organic pollutants from wastewater, J. Environ. Manag. 113 (2012) 170–183.
[5] M.A. Shannon, P.W. Bohn, M. Elimelech, J.G. Georgiadis, B.J. Mariñas, A.M. Mayes, Science and technology for water purification in the coming decades, Nature 452 (2008) 301–310.

[6] T. Robinson, G. McMullan, R. Marchant, P. Nigam, Remediation of dyes in textile effluent: A critical review on current treatment technologies with a proposed alternative, Bioresour. Technol. 77 (2001) 247–255.
[7] M. Sundararajan, S.K. Ghosh, Designing novel materials through functionalization of carbon nanotubes for application in nuclear waste management: Speciation of Uranyl, J. Phys. Chem. A 115 (2011) 6732–6737.
[8] J. Yuan, X. Liu, O. Akbulut, J. Hu, S.L. Suib, J. Kong, F. Stellacci, Superwetting nanowire membranes for selective absorption, Nature Nanotechnol. 3 (2008) 332–336.
[9] G. Xi, J. Ye, Ultrathin SnO_2 nanorods: Template- and surfactant-free solution phase synthesis, growth mechanism, optical, gas-sensing, and surface adsorption properties, Inorg. Chem. 49 (2010) 2302–2309.
[10] K.P. Shubha, C. Raji, T.S. Anirudhan, Immobilization of heavy metals from aqueous solutions using polyacrylamide grafted hydrous tin(IV) oxide gel having carboxylate functional groups, Water Res. 35 (2001) 300–310.
[11] Y.F. Zeng, Z.L. Liu, Z.Z. Qin, Decolorization of molasses fermentation wastewater by SnO_2-catalyzed ozonation, J. Hazard. Mater. 162 (2009) 682–687.
[12] L. Shi, H. Lin, Facile fabrication and optical property of hollow SnO_2 spheres and their application in water treatment, Langmuir 26 (2010) 18718–18722.
[13] Z. Wei, R. Xing, X. Zhang, S. Liu, H. Yu, P. Li, Facile template-free fabrication of hollow nestlike α-Fe_2O_3 nanostructures for water treatment, ACS Appl. Mater. Interfaces 5 (2013) 598–604.
[14] W. Cai, J. Yu, B. Cheng, B. Su, M. Jaroniec, Synthesis of boehmite hollow core/shell and hollow microspheres via sodium tartrate-mediated phase transformation and their enhanced adsorption performance in water treatment, J. Phys. Chem. C 113 (2009) 14739–14746.
[15] M. Chen, C. Ye, S. Zhou, L. Wu, Recent advances in applications and performance of inorganic hollow spheres in devices, Adv. Mater. 25 (2013) 5343–5351.
[16] W. Konicki, K. Cendrowski, X.C. Chen, E. Mijowska, Application of hollow mesoporous carbon nanospheres as an high effective adsorbent for the fast removal of acid dyes from aqueous solutions, Chem. Eng. J. 228 (2013) 824–833.
[17] Z.Y. Zhong, Y.D. Yin, B. Gates, Y.N. Xia, Preparation of mesoscale hollow spheres of TiO_2 and SnO_2 by templating against crystalline arrays of polystyrene beads, Adv. Mater. 12 (2000) 206–209.
[18] X.W. Lou, Y. Wang, C. Yuan, J.Y. Lee, L.A. Archer, Template-free synthesis of SnO_2 hollow nanostructures with high lithium storage capacity, Adv. Mater. 18 (2006) 2325–2329.
[19] J.S. Chen, C.M. Li, W.W. Zhou, Q.Y. Yan, L.A. Archer, X.W. Lou, One-pot formation of SnO_2 hollow nanospheres and α-Fe_2O_3@SnO_2 nanorattles with large void space and their lithium storage properties, Nanoscale 1 (2009) 280–285.
[20] F. Gyger, M. Hübner, C. Feldmann, N. Barsan, U. Weimar, Nanoscale SnO_2 hollow spheres and their application as a gas-sensing material, Chem. Mater. 22 (2010) 4821–4827.
[21] X. Sun, J. Liu, Y. Li, Use of carbonaceous polysaccharide microspheres as templates for fabricating metal oxide hollow spheres, Chem. A Eur. J. 12 (2006) 2039–2047.
[22] J.S. Chen, X.W. Lou, SnO_2-based nanomaterials: Synthesis and application in lithium-ion batteries, Small 9 (2013) 1877–1893.
[23] H.M. Cai, S.Z. Ren, M. Wang, C.Y. Jia, Preparation and properties of monodisperse SnO_2 hollow micro/nano spheres, Acta Phys. -Chim. Sin. 29 (2013) 881–888.
[24] X. Sun, Y. Li, Colloidal carbon spheres and their core/shell structures with noble-metal nanoparticles, Angew. Chem. Int. Ed. 43 (2004) 597–601.
[25] Z. Yang, Z. Niu, Y. Lu, Z. Hu, C.C. Han, Templated synthesis of inorganic hollow spheres with a tunable cavity size onto core-shell gel particles, Angew. Chem. Int. Ed. 42 (2003) 1943–1945.
[26] X. Lu, D. Zheng, J. Gan, Z. Liu, C. Liang, P. Liu, Y. Tong, Porous CeO_2 nanowires/nanowire arrays: Electrochemical synthesis and application in water treatment, J. Mater. Chem. 20 (2010) 7118–7122.
[27] X. Lu, D. Zheng, P. Zhang, C. Liang, P. Liu, Y. Tong, Facile synthesis of free-standing CeO_2 nanorods for photoelectrochemical applications, Chem. Commun. 46 (2010) 7721–7723.
[28] X. Zhuang, Y. Wan, C. Feng, Y. Shen, D. Zhao, Highly efficient adsorption of bulky dye molecules in wastewater on ordered mesoporous carbons, Chem. Mater. 21 (2009) 706–716.
[29] J. Qu, D. Zheng, X. Lu, J. Shi, C. Lan, Electrochemical assembling of aligned porous $Nd(OH)_3$ nanobelts with high performance in water treatment, Inorg. Chem. Commun. 13 (2010) 1425–1428.
[30] Y. Liu, J. Shi, Q. Peng, Y. Li, Self-assembly of ZnO nanocrystals into nanoporous pyramids: High selective adsorption and photocatalytic activity, J. Mater. Chem. 22 (2012) 6539–6541.
[31] N. Li, K. Du, G. Liu, Y.P. Xie, G.M. Zhou, J. Zhu, F. Li, H.M. Cheng, Effects of oxygen vacancies on the electrochemical performance of tin oxide, J. Mater. Chem. A 1 (2013) 1536–1539.